

CKD-516 displays vascular disrupting properties and enhances anti-tumor activity in combination with chemotherapy in a murine tumor model

Chang Hoon Moon · Seung Ju Lee · Ho Yong Lee ·
Le Thi Kim Dung · Wha Ja Cho · HeeJeong Cha ·
Jeong Woo Park · Young Joo Min

Received: 8 August 2013 / Accepted: 17 October 2013 / Published online: 8 November 2013
© Springer Science+Business Media New York 2013

Summary Purpose CKD-516 is a benzophenone analog in which the B ring is modified by replacement with a carbonyl group. The study assessed CKD-516 as a vascular disrupting agent or anti-cancer drug. **Methods** To assess the effect of S516 on vascularization, we analyzed the effect on human umbilical vein endothelial cells (HUVECs). To determine the inhibition of cell proliferation of S516, we used H460 lung carcinoma cells. The alteration of microtubules was analyzed using immunoblot, RT-PCR and confocal imaging. To evaluate the anti-tumor effects of gemcitabine and/or CKD-516, H460 xenograft mice were treated with CKD-516 (2.5 mg/kg) and/or gemcitabine (40 mg/kg), and tumor growth was compared with vehicle-treated control. For histologic analysis, liver, spleen and tumor tissues from H460 xenograft mice were obtained 12 and 24 h after CKD-516 injection. **Results** Cytoskeletal changes of HUVECs treated with 10 nM S516 were assessed by immunoblot and confocal imaging. S516 disrupted tubulin assembly and resulted in microtubule

dysfunction, which induced cell cycle arrest (G2/M). S516 markedly enhanced the depolymerization of microtubules, perhaps due to the vascular disrupting properties of S516. Interestingly, S516 decreased the amount of total tubulin protein in HUVECs. Especially, S516 decreased mRNA expression α -tubulin (HUVECs only) and β -tubulin (HUVECs and H460 cells) at an early time point (4 h). Immunocytochemical analysis showed that S516 changed the cellular microtubule network and inhibited the formation of polymerized microtubules. Extensive central necrosis of tumors was evident by 12 h after treatment with CKD-516 (2.5 mg/kg, i.p.). In H460 xenografts, CKD-516 combined with gemcitabine significantly delayed tumor growth up to 57 % and 36 % as compared to control and gemcitabine alone, respectively. **Conclusion** CKD-516 is a novel agent with vascular disrupting properties and enhances anti-tumor activity in combination with chemotherapy.

Keywords CKD-516 · Microtubule · Vascular-disrupting agent

C. H. Moon · S. J. Lee · H. Y. Lee · L. T. K. Dung · W. J. Cho ·
Y. J. Min (✉)
Biomedical Research Center, Ulsan University Hospital, University
of Ulsan College of Medicine, 290-3 Jeonha-dong, Dong-gu,
Ulsan 682-060, Republic of Korea
e-mail: yjmin65@gmail.com

Y. J. Min
Division of Hematology-Oncology, Department of Internal
Medicine, Ulsan University Hospital, University of Ulsan College of
Medicine, Ulsan 682-060, Republic of Korea

H. Cha
Department of Pathology, Ulsan University Hospital, University of
Ulsan College of Medicine, Ulsan 682-060, Republic of Korea

J. W. Park
Department of Biological Sciences, University of Ulsan,
Ulsan 680-749, Republic of Korea

Introduction

Tumor neovasculature is an important target in cancer therapy, as the growth and locoregional or systemic metastasis of tumors depend on vascular network [1, 2]. As cancer cells proliferate, their demands for nutrients and oxygen increase. To recruit new blood vessels to the growing tumor, cancer cells secrete various angiogenic factors [3]. The generation of tumor neovasculature to support tumor growth is thought to result from the sprouting of microvessels from pre-existing blood vessels in the host organ [1, 4], or from the differentiation of endothelial cell precursors largely mobilized from the bone marrow [5, 6].

Vascular disrupting agents (VDAs) present an alternative way to target tumor blood vessels. A VDA has a different mechanism from anti-angiogenic drugs like bevacizumab, sunitinib and sorafenib. VDAs damage established tumor blood vessels. VDAs comprise two major groups: microtubule binding agents and flavonoids. These can be subgrouped as agents that bind to the colchicine binding site in tubulin and result in the depolymerization of microtubules [7], leading to the disruption of the endothelial cytoskeleton with the ultimate shutdown of blood flow, which causes tumor necrosis within a few hours of administration [8, 9].

Microtubules are dynamic structures composed of α - β tubulin heterodimers that organize the cytoplasm during interphase and segregate condensed chromosomes during mitosis. Anti-mitotic drugs that interfere with the microtubule system are key components of combination chemotherapies for the treatment of carcinomas [9, 10].

Microtubule-targeting agents are some of the most effective chemotherapeutic agents used in the clinic today. These drugs comprise microtubule stabilizers and microtubule depolymerizers [10, 11]. Although these two classes are differentiated by their effects on interphase microtubules, all microtubule-active drugs effectively kill cancer cells by a common mechanism of inhibiting microtubule dynamics, leading to mitotic defects and subsequent apoptosis [12].

The Chong Kun Dang Research Institute (Suwon, Korea) has been developing anticancer drugs that target tubulin with benzophenone scaffold. This effort culminated in a discovery of a novel tubulin polymerization inhibitor designated compound 65 (CKD-516). CKD-516 is a valine prodrug of 22 (S516) and is a benzophenone analog with a modification of the B ring, which is replaced by a carbonyl group [13]. Compound 22 exhibits potent cytotoxicity against several cancer cells including the P-gp overexpressing MDR positive HCT15 cell line. It also induces cell cycle arrest at G2/M phase, which is associated with strong inhibition of tubulin polymerization. In vivo efficacy was improved by preparing the (L)-valine prodrug, 65 (CKD-516), which, together with greatly improved aqueous solubility, exhibits potent antitumor efficacy against both murine tumors (CT26 and 3LL) and human xenografts (HCT116 and HCT15) in mice [13].

Here, we report the vascular disrupting effects of CKD-516 in H460 xenograft mice. CKD-516 did not affect blood supply to normal organs including liver and kidneys, and so had selective effects on tumor vessels. Use of human umbilical vein endothelial cells (HUVECs) supported the view that the vascular disrupting effect of CKD-516 results from the morphologic change of endothelial cells by degradation of microtubules. Our results implicate CKD-516 as a new VDA that in combination with gemcitabine enhances the anti-tumor activity in H460 xenograft mice.

Materials and methods

Cell culture and reagents

HUVECs were purchased from ATCC (Manassas, VA, USA) and were maintained in Ham's Kaighn's Modification F12 (F12K; Invitrogen, Carlsbad, CA, USA) supplemented with 2 mM L-Glutamine (Invitrogen) and 0.1 mg/ml heparin sodium salt from porcine intestinal mucosa (Sigma-Aldrich, St. Louis, MO, USA), 0.05 mg/ml Endothelial Cell Growth Supplement (ECGS; BD, Franklin Lakes, NJ, USA) and 10 % fetal bovine serum (FBS; Invitrogen). The medium was prepared fresh every 2 weeks. H460 lung cancer cell line (ATCC) was grown in RPMI 1640 medium supplemented with 10 % FBS. All cell lines were maintained in a 5 % CO₂ incubator at 37 °C. S516 was obtained from the Chong Kun Dang Research Institute and 100 μ M stock solutions were prepared in H₂O. Aliquots of the stock were stored at -20 °C. The stock solutions were stable for over 6 months. Working concentrations were freshly prepared daily by diluting the stock with complete media. Gemcitabine (Eli Lilly, Indianapolis, IA, USA) was prepared at an 80 mg/ml concentration in phosphate buffered saline (PBS).

In vitro tubulin polymerization assay

The effects of CKD-516 on the microtubule assembly-disassembly process were determined using a tubulin polymerization kit (Cytoskeleton, Denver, CO, USA). Purified bovine brain tubulin was resuspended on ice in ice-cold buffer (80 mM PIPES at pH 6.9, 2 mM MgCl₂, 0.5 mM EGTA, 15 % glycerol, 1 mM GTP) and 100 μ l of the suspension (3 mg/ml) was added to half of a 96-well plate pre-warmed to 37 °C as per the manufacturer's instruction. The assay was determined by measuring the change of absorbance (340 nm) at room temperature using an uQuant spectrophotometer every 5 min for 70 min (Bio-Tek Instruments, Winooski, VT, USA).

Animals and tumor model

All research was governed by the principles of the Guide for the Care and Use of Laboratory Animals and approved by the University of Ulsan Animal Care and Use Committee. Female Balb/c nude mice (4–6 weeks of age) were obtained from Orient Bio (Seoul, Korea) and were maintained under specific pathogen-free conditions.

Histological analysis

H460 cells were harvested from monoconfluent monolayer cell cultures in 1x PBS and 2 \times 10⁶ cells in a total volume of 100 μ l and were injected subcutaneously. When the tumor

size became 3 mm in diameter, the control group was injected with PBS, while the experimental group was intraperitoneally injected with 100 μ l of CKD-516 at a concentration of 2.5 mg/kg. At 12 and 24 h after injection, the liver, kidney and tumor tissues were acquired and put into a 37 % solution of formaldehyde for 24 h. The tissues were inserted into paraffin and sectioned at a thickness of 4 μ m using a microtome (SLEE MAINZ GmbH, Germany). The sections were placed on slides and stained with Mayer's hematoxylin and eosin Y (both from Sigma-Aldrich, St. Louis, MO, USA). Images were observed using a model BX50 inverted microscope (Olympus, Tokyo, Japan).

Cytotoxicity assay

The cytotoxicity assay used to determine drug-mediated cytotoxicity utilized 3-(4,5-dimethylthiazol-2-yl)-5-(3-carboxymethoxyphenyl)-2-(4-sulfophenyl)-2H-tetrazolium (MTS) reagent that was part of the Cell Titer 96 Aqueous One Solution (Promega, Madison, WI, USA). Absorption was measured at 490 nm. Briefly, the assay entailed seeding HUVECs at 0.5×10^5 cells per well for 24 h at 37 °C and 5 % CO₂. After addition of the drugs at the indicated concentrations, the cells were incubated for either 24 or 48 h. Twenty microliters of the MTS solution was added to each well and incubated at 37 °C for 4 h. Thereafter, absorbance values (A) for each well were measured using a microplate spectrophotometer (Bio-Tek Instruments). The percentage of viable cells was calculated using the background-corrected absorbance using the following calculation: % cytotoxicity = $(1 - A \text{ of experimental well} / A \text{ of positive control well}) \times 100$.

Flow cytometry

Cells (2×10^6) were treated with each drug at the indicated concentration for 24 h. Cells were washed with PBS by spinning at 1,000 rpm for 5 min at 4 °C and fixed with 1 ml of ice-cold 95 % ethanol drop-wise while vortexing. The fixed cells were incubated on ice for at least 30 min and then washed as described above. The pellets were resuspended in 1 ml PBS and 100 μ l of a 1 mg/ml propidium iodide (PI) stock was added for 5–10 min at room temperature. Flow cytometry was performed using a FACSCalibur flow cytometer and Cell Quest software (BD Biosciences, Franklin Lakes, NJ, USA).

Immunoblots

Cells grown to 70 %–80 % confluence in a F25 culture flask were harvested after drug treatment in 100 μ l/well of protein lysis buffer containing 50 mM Tris, pH 7.5, 150 mM NaCl, 1 % NP-40, 0.5 % sodium deoxycholate, 0.1 % sodium dodecyl sulfate (SDS), and protease inhibitor (protease

inhibitor cocktail tablets; Roche, Basel Switzerland) plus 200 units/ml aprotinin (Sigma-Aldrich) and 10 μ mol/l trichostatin A (Cayman Chemical, Ann Arbor, MI, USA). Protein concentrations were determined using a commercial protein assay reagent (Bio-Rad, Hercules, CA, USA) and 3 μ g protein were loaded into each well and resolved using 10 % sodium dodecyl sulfate-polyacrylamide gel electrophoresis (SDS-PAGE). After protein transfer onto nitrocellulose, blots were blocked using 5 % milk and each blot was probed with anti-glyceraldehyde 3-phosphate dehydrogenase (GAPDH) (Santa Cruz Biotechnology, Santa Cruz, CA, USA) as an internal control. Other primary antibodies used were anti- α -tubulin (Santa Cruz Biotechnology) and the membrane was reacted with goat anti-mouse IgG secondary antibody (Santa Cruz Biotechnology) conjugated to horseradish peroxidase (HRP) and exposed to light with Molecular Imager ChemiDoc XRS (Bio-Rad) using Immun-Star™ and quantified by a Quantity One Image analyzer (Bio-Rad).

Reverse transcription-polymerase chain reaction (RT-PCR) HUVECs were cultivated in F25 culture flasks containing F-12 K medium (Sigma-Aldrich) supplemented with 10 % FBS and ECGS (Sigma-Aldrich). After cultivation for 24 h, the cells were treated with 5 nM, 10 nM and 50 nM S516. At 6 and 48 h after the treatment, the cells were collected. Total RNA was extracted using Trizol (Invitrogen) from the collected cells using alcohol precipitation. One microgram of total RNA was reverse transcribed. PCR was performed on cDNA template using Taq polymerase (Bioneer, Seoul, Korea) and the following primers: α -tubulin (sense: 5'-ATT GTG CCT TCA TGG TAG AC-3', antisense: 5'-TTC TGT CAG GTC AAC ATT CA-3'), β -tubulin (sense: 5'-AAC GAC CTC GTC TCT GAG TA-3', antisense: 5'-AAT TCT GAG GGA GAG GAA AG-3') and GAPDH (sense: 5'-ACC ACT TTG TCA AGC TCA TT-3', antisense: 5'-AGT GAG GGT CTC TCT CTT CC-3'). The PCR product was confirmed by 1.5 % agarose gel electrophoresis.

Immunofluorescence and confocal microscopy

HUVECs (or other cancer cells) were cultured on a confocal dish (SPL, Seoul, Korea) with F-12 K (Sigma-Aldrich) medium containing 10 % FBS and endothelial cell growth supplement (ECGS, E2759; Sigma-Aldrich). After cultivation for 24 h, the cells were treated with S516 at concentrations of 5 nM, 10 nM or 50 nM. At 24 h (cancer cells) or 48 h after the treatment, the cells were fixed with 3.7 % paraformaldehyde at the room temperature for 10 min. After being washed with PBS solution three times, the cells were treated with 0.15 % Triton X-100 for 15 min and washed three times with PBS. After being blocked with 2 % bovine serum albumin (BSA, Sigma-Aldrich) at room temperature for 60 min, the cells were

also washed three times with PBS. Monoclonal antibody against α -tubulin (Santa Cruz Biotechnology, Santa Cruz, CA, USA) was used to react with cell tubulin at room temperature for 1 h and the cells were washed three times with PBS. They were reacted with rat anti-mouse IgG1 secondary antibody (BD Bioscience) conjugated to fluorescein isothiocyanate (FITC). After being washed three times with PBS, the cells were analyzed using a model FV500 confocal laser scanning microscope (Olympus, Tokyo, Japan).

Anti-tumor activity

Anti-tumor effects of gemcitabine or CKD-516 were evaluated in a H460 xenograft model. Female BALB/c nude mice weighing approximately 20 g were inoculated by subcutaneous injection with 2×10^6 of H460 cells per mouse. When tumors reached 3–4 mm in diameter, the control group was injected weekly with PBS. The experimental groups were divided into a group injected with 100 μ l of gemcitabine (40 mg/kg/week, for 4 weeks) and the other group was injected with 100 μ l of both CKD-516 (2.5 mg/kg/week, for 4 weeks). Mice were monitored for toxicity by body weight measurements and tumor growth was measured once every 2 days using calipers throughout the experimental period. Tumor volumes were calculated based on the following formula: tumor volume=(length \times width²) \times $\pi/6$. In a combination experiment, when the tumor size reached 3–4 mm in diameter, mice were randomized into different treatment groups: gemcitabine alone (40 mg/kg/week), gemcitabine (40 mg/kg) combined with CKD-516 (2.5 mg/kg) and vehicle control (PBS). All experiment groups were treated weekly for 4 weeks.

Statistical analysis

The results obtained from at least three independent experiments were expressed as mean \pm standard deviation. One-way ANOVA test were used to determine the differences between control and treatment groups. $P < 0.001$ was considered to be statistically significant. All data were analyzed using GraphPad software.

Results

Effects of S516 on in vitro tubulin polymerization

CKD-516 is a prodrug which becomes an active drug, S516, after being cleaved by endogenous protease (Fig. 1a).

In vitro polymerization assays with pure tubulin were conducted in the presence of drugs to further test the possibility that S516 directly destabilizes microtubules (Fig. 1b). Pure tubulin derived from bovine brain was mixed

with or without drug in GTP-containing polymerization buffer. Samples were incubated at 37 °C for 60 min to polymerize microtubule, and then were analyzed. As shown in Fig. 1b, S516 (4 and 10 μ M) and vincristine (10 μ M) completely blocked microtubule polymerization. It is important to compare the effect of each drug to that of its vehicle, which was water for paclitaxel and dimethylsulfoxide (DMSO) for S516; microtubule polymerization was promoted in the vehicle containing preparations. Thus, this data suggest that S516 has directly binds tubulin and induces tubulin depolymerization.

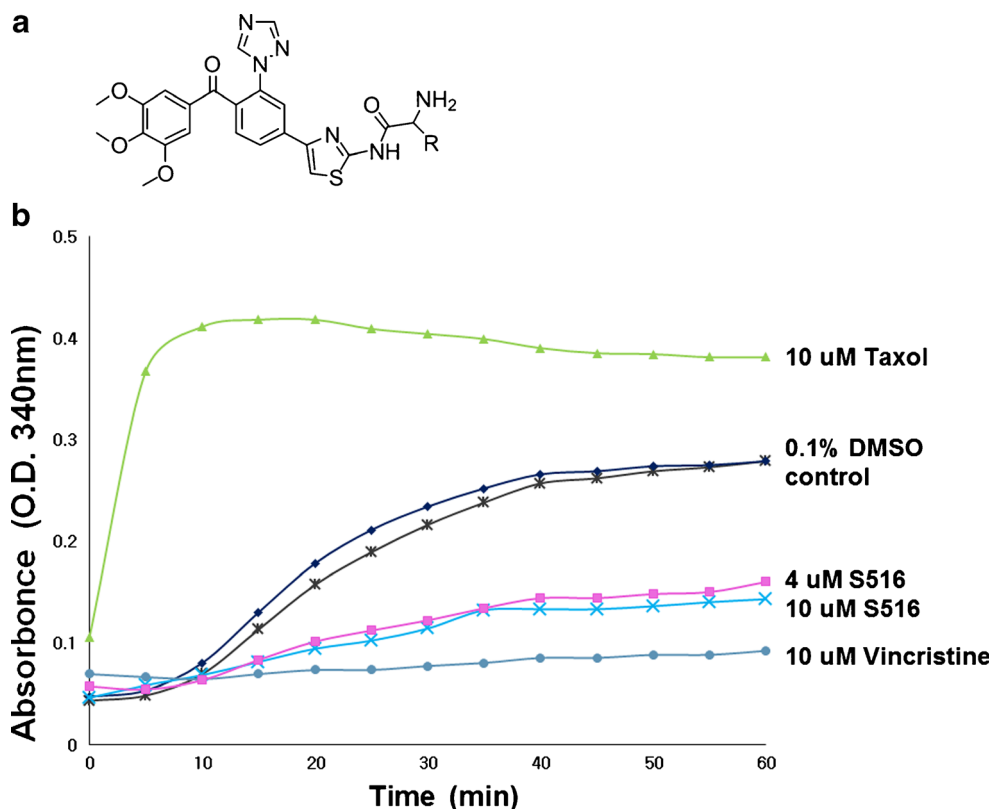
Effect of S516 on cancer cells growth and G2/M arrest

We examined different concentrations of S516 and measured the cytotoxicity on various cancer cell lines using the MTS assay after 24 and 48 h of treatment. As shown in Fig. 2a, although S516 exhibited in vitro cytotoxic activity on tested cell lines, it was not dose-dependent. Interestingly, the inhibition of cell growth was maintained at a similar level, with no further inhibition. We next examined whether the inhibition of cell growth by S516 could cause cell cycle arrest. After H460 cells were treated with indicated concentrations of S516 for 24 h, S516-induced cell cycle arrest was analyzed by fluorescence-activated cell sorting (FACS) and compared with control for 40 nM paclitaxel and 40 nM vincristine treatments. As shown in Fig. 2b, paclitaxel and vincristine induced G2/M phase arrest (72 % and 71.5 %, respectively). At a low concentration (5 nM S516), <28 % of cells were in the G2/M phase, but at S516 concentrations >10 nM, >84 % of cells were in the G2/M phase. These data indicate that S516-induced cell death was preceded by cell cycle arrest in the G2/M phase.

Effects of S516 on cellular tubulin polymerization

To investigate whether cell death was caused by a cytoskeletal abnormality, which is important for cell division and cell differentiation, the change in α -tubulin expression in the cytoskeleton was identified by the division of tubulin into the isolated form (soluble, S) and polymerized form (ppt, P). This procedure and subsequent modifications have been widely-used and allow a quick and consistent assessment of the proportion of tubulin polymer in cells under a variety of experimental conditions. An increase in the S fraction served as an indicator of destabilized tubulin. As shown in Fig. 3, vincristine or paclitaxel enhanced the cellular levels of the S fraction or P fraction in the cell lysates. When cells were treated with S516, the amount of tubulin in the depolymerized fraction, S, was increased compared with control cell lysate. The tubulin shift to the S fraction was noted over 10–20 nM S516. As such, the increase in the number of cells in arrest with S516 found in the cell death experiment correlated with

Fig. 1 Effect of S516 on microtubule polymerization in vitro. **a** Chemical structure of a CKD-516 **b** Purified tubulin from bovine brain tissue (cytoskeleton) was incubated at 37 °C in reaction mixtures containing 1 mM GTP, 10 μM paclitaxel (Taxol), 10 μM vincristine, 4 and 10 μM S516 and the mock-treated solution as control. Tubulin polymerization was determined by measuring the absorbance at 340 nm



the increased S fraction of tubulin. These data indicated that S516 induces tubulin depolymerization in dose- and time-dependent manners.

Effect of S516 on microtubule stability and the total amount

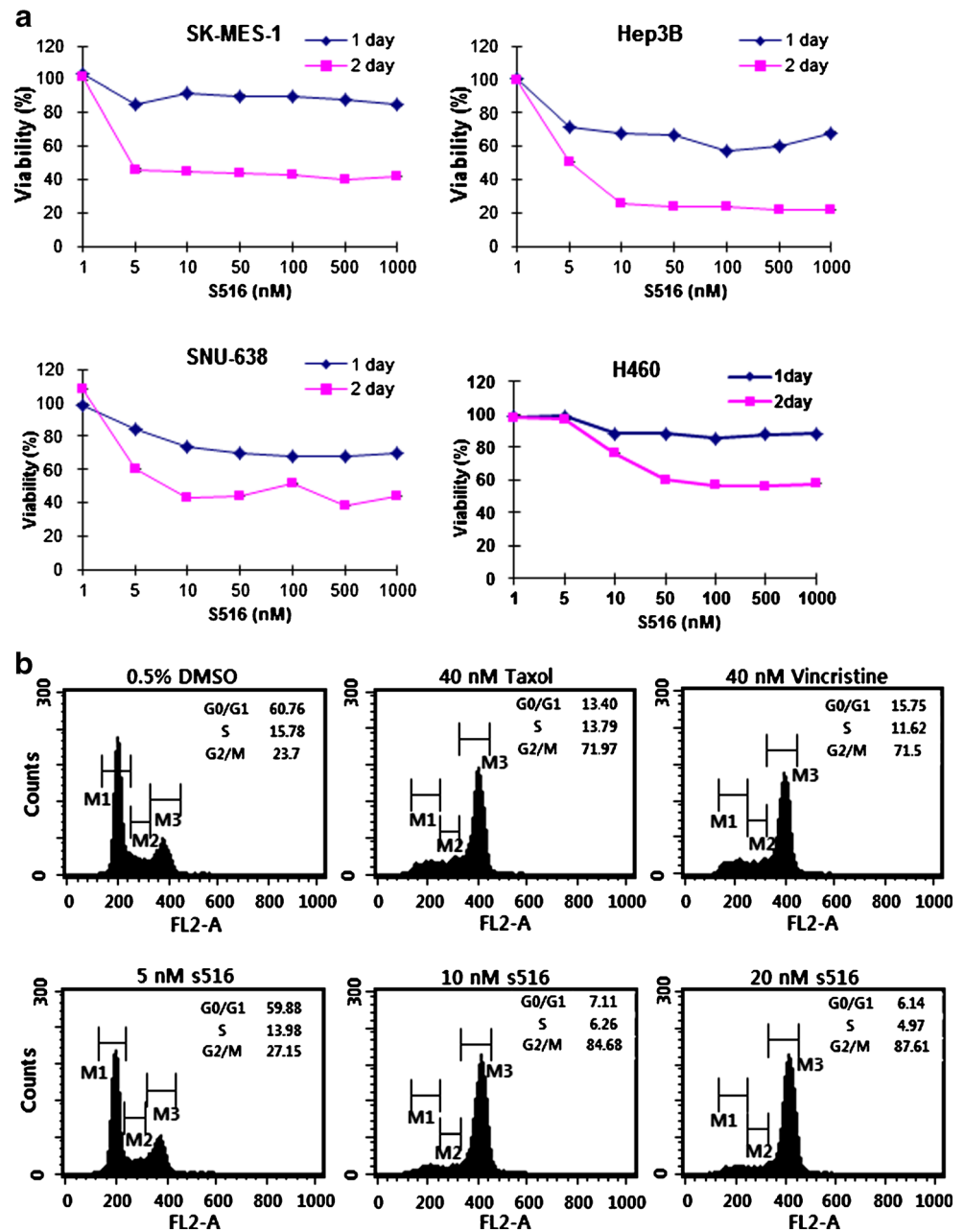
It is well established that tubulin can be altered by posttranslational modifications, and several of these are exclusive to α -tubulin. Although the precise relationship between these tubulin modifications and microtubule stability has not been elucidated, several changes are definitive markers of microtubule stability [14, 15]. Therefore, we examined the acetylation of α -tubulin. As shown in Fig. 4a, a marked increase in the amount of acetylated α -tubulin was evident in paclitaxel-treated lysate, compared to the control. But S516-treated lysate was decreased compared to the control. In addition, to check the change in the overall expression of tubulin, the total amount of tubulin protein was identified by Western blotting. S516 concentrations >10 nM reduced the protein level of α -tubulin and β -tubulin (Fig. 4a), supporting the idea that S516 drives the specific destruction of α -tubulin and β -tubulin proteins. We also determined the cellular gene expression level by RT-PCR. Interestingly, β -tubulin mRNA level was decreased at 4 h and α -tubulin was decreased 24 h after treatment of S516 at each concentration (Fig. 4b). Since S516 treatment resulted in the destabilization of tubulin, we tested whether S516

treatment affected the cellular microtubule network by confocal microscopy. Cells treated with S516 displayed a reduced total amount of microtubules and the microtubule network was disrupted, depending on the S516 concentration (Fig. 4c). These data indicated that the quantitative change in the protein of α -tubulin and β -tubulin was not caused by the change in the expression of mRNA, but rather resulted from the change in the level of the protein. These results occurred independent of each other.

Analysis of G2/M arrest and cytotoxicity of HUVECs by S516

To assess the effect of S516 on vascularization, we first analyzed the effect on endothelial cells, which are important for vascularization. As shown in Fig. 5a, although S516 exhibited in vitro cytotoxic activity on HUVECs, it was also not dose-dependent. The inhibition of HUVECs growth was maintained at a similar level, with no further inhibition. We next examined whether the inhibition of cell growth by S516 could cause cell cycle arrest. After HUVECs were treated with indicated concentrations of S516 for 48 h, 72 h and 96 h, S516-induced cell cycle arrest was analyzed by FACS and compared with control (0.1 % DMSO) and 40 nM vincristine treatments. As shown in Fig. 5b, vincristine induced G2/M phase arrest (16.9 % at 96 h). At a low concentration (10 nM S516) and early time point, <14 % of cells were in the G2/M

Fig. 2 Effect of S516 on cancer cell growth and G₂/M arrest. **a** To show the inhibitory effects of S516 on the cell proliferation, exponentially growing cells were treated with the indicated concentrations of S516 for 24 h and 48 h, and cell proliferation was assessed by using the MTS reagent. Cytotoxic effect of S516 was increased in a time-dependent manner. **b** To observe the G₂/M arrest of S516, H460 cells were treated either vehicle (control) or each concentration of S516 and paclitaxel for 24 h. Cells were analyzed by flow cytometry and the percentage of cells in each phase of the cell cycle was analyzed using flow cytometry. The analysis showed significantly increased the G₂/M phase in S516-treated cells



phase, but at a concentration of 50 nM S516 and late time point, >24 % of cells were in the G₂/M phase. These data also indicate that although S516 has weak cytotoxicity on HUVECs, S516-induced cell death was preceded by cell cycle arrest in the G₂/M phase.

S516 induces microtubule depolymerization in HUVECs

We also determined whether the inhibition of cell growth was caused by a cytoskeletal abnormality in HUVECs. At a concentration of >10 nM S516, the amount of tubulin in the depolymerized fraction, S, was increased compared with control cell lysate (Fig. 6a). To check the change in the overall

expression of tubulin, the total amount of tubulin protein was identified by Western blotting. As shown in Fig. 6b, at a concentration of >5 nM S516 and 24 h reduced the protein level of β -tubulin but α -tubulin protein was reduced at 48 h (Fig. 6b), supporting the idea that S516 drives the specific destruction of α -tubulin and β -tubulin proteins was reduced starting at 48 h and at >10 nM S516. We also determined the HUVEC gene expression level by RT-PCR. Interestingly, α -tubulin and β -tubulin mRNA level were decreased at 4 h, but both mRNA level were recovered at 48 h after the treatment of S516 (Fig. 6c). Since S516 treatment resulted in the destabilization of tubulin, we also tested whether S516 treatment affected the cellular microtubule network by

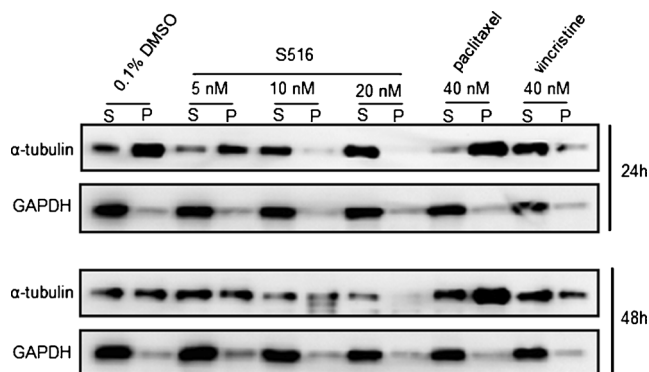


Fig. 3 The effects of S516 on cellular tubulin polymerization. H460 cells were treated with S516, or DMSO as the control, for 24 h and 48 h at the indicated concentrations. Cell lysates were separated into polymerized (P) or soluble (S) fractions by centrifugation 2,000 rpm at 22 °C for 30 min. Equal volumes were separated by SDS-PAGE and evaluated by immunoblot probed with anti- α -tubulin antibody and anti-GAPDH antibody

confocal microscope. Cells treated with S516 displayed a reduced total amount of microtubules, depending on the S516 concentration (Fig. 6d). These data indicated that the quantitative change in the protein of α -tubulin and β -tubulin was not caused by the change in the expression of mRNA. These results also occurred independent of each other.

Gross morphological and histopathological changes

Figure 7a illustrates the gross tumor morphology after injection of CKD-516 (2.5 mg/kg). While the discoloration of tumors of the mice injected with PBS was observed after 3 weeks, tumors of the mice injected with CKD-516 became discolored on day 10 after the injection of CKD-516. With time, the tumors became discolored regardless of the injection of CKD-516. The sequential histopathological changes after drug treatment are shown in Fig. 7b. In tumor tissues of nude mice who did not receive CKD-516, the cell density remained constant and the cells were distributed without any change in shape. On the contrary, when the exposure time of CKD-516 (2.5 mg/kg) increased, the scope of necrotic cell death in the tumor tissues of mice injected with CKD-516 increased and necrotic cell death was evident in the central part of the tumors. In liver and kidney tissues, CKD-516-mediated ischemic damage was not observed.

Anti-tumor activity of CKD-516 in the H460 xenograft model

To evaluate the anti-tumor effects of CKD-516 alone, H460 xenograft mice were treated with CKD-516 (2.5 mg/kg) and tumor growth was compared with vehicle-treated control. CKD-516 alone treatment did not delay the progression of tumor growth (Fig. 8a). This data suggested that CKD-516

alone has no inhibitory effect on tumors in the H460 xenograft model.

Gemcitabine combined with CKD-516 has an additive inhibitory effect in the H460 xenograft model

Since gemcitabine is a chemotherapeutic agent that is widely-used in lung cancer and several other solid tumors, we choose gemcitabine as a combination partner in this study. To evaluate the anti-tumor effects of gemcitabine treatment alone or in combination with CKD-516, we used only one sequence of administration. One group was injected with 100 μ l of gemcitabine at the concentration of 40 mg/kg and a second group was injected with 100 μ l of CKD-516 (2.5 mg/kg) and gemcitabine (40 mg/kg) at defined times. Twenty four hours after being injected with gemcitabine, xenograft mice were injected with CKD-516 (Fig. 8b). All treatments were administrated once weekly for 4 weeks. Compared to the administration of gemcitabine alone, CKD-516+gemcitabine produced >1.5-fold increase in tumor inhibition. In the H460 xenograft model, growth was inhibited with gemcitabine alone as compared to control (33.0 %). However, xenograft mice treated with CKD-516 and gemcitabine showed a significantly tumor growth delay (57 % and 36 %) as compared to control and gemcitabine alone. In combining the two agents, the growth delay was highly significant, with almost a doubling of the delay noted for gemcitabine alone, and was much than would be expected from the summation of the growth delays of the two agents administered separately. This suggests that the effects observed were additive (Fig. 8b).

Discussion

In this study, we directly compared the effect of S516 on HUVECs (vascular endothelial cells) and H460 cells (lung carcinoma cells). We felt that the comparison was important to decide the direction of the development of CKD-516 as a VDA or an anti-cancer drug.

VDAs have shown much promise pre-clinically as anti-cancer therapeutics, and a small number are currently being investigated in clinical trials. However, the failure of such agents to target the peripheral tumor rim means that their efficacy as a single-agent therapeutic strategy is in need of improvement [16]. One revised strategy involves treatment in combination with standard chemotherapeutic agent that can destroy the remaining tumor cells. There have been several pre-clinical studies that have demonstrated improved efficacy [17].

The biological response of tumors to VDA treatment is typically characterized by early increases in vascular permeability followed by vascular collapse and cessation of blood flow leading to ischemia and tumor necrosis [18–20].

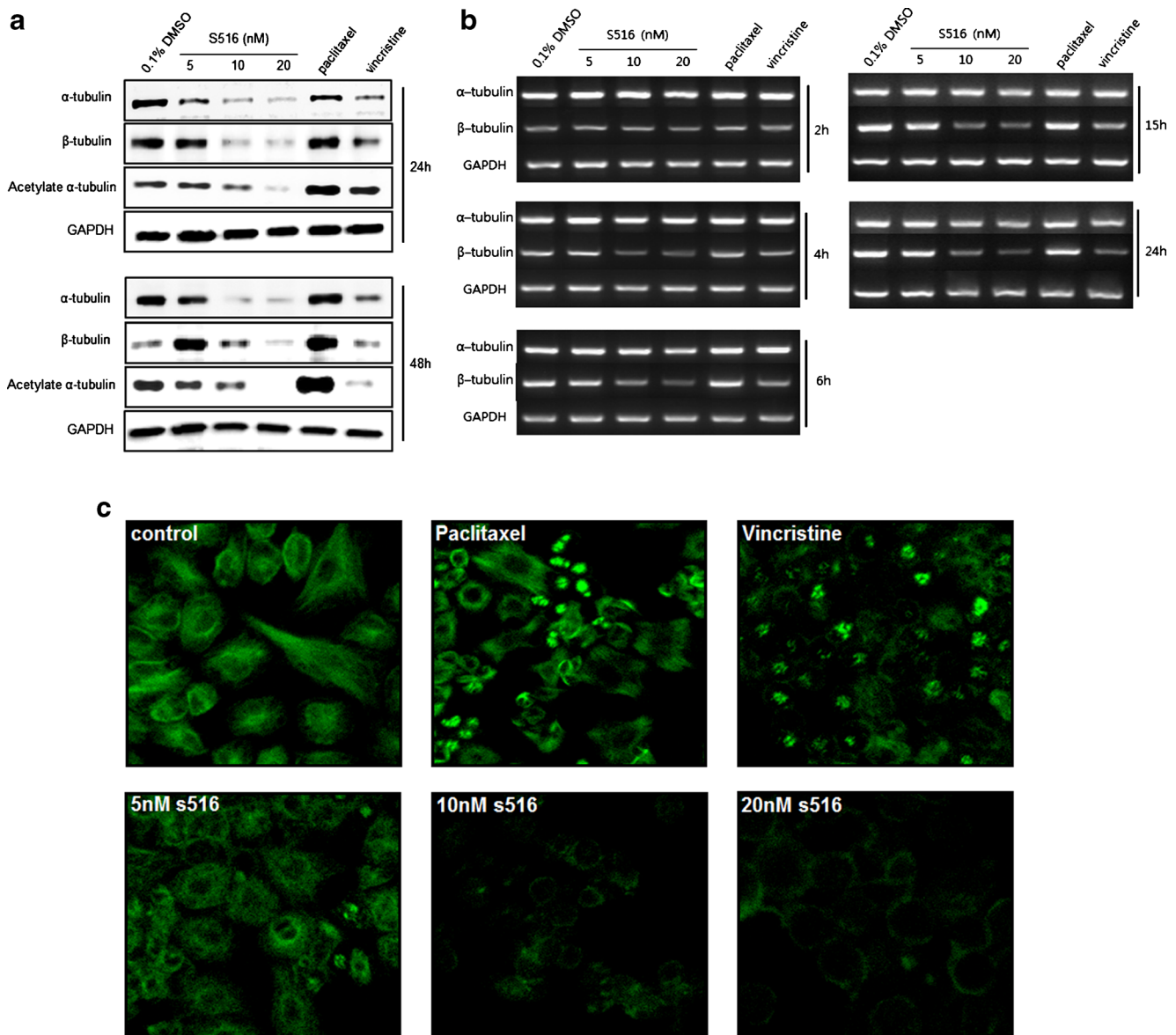


Fig. 4 S516 promotes degradation of α - and β -tubulin in H460 cells. **a** Immunoblot of H460 cells treated with S516 (5, 10 and 20 nM) for 24 h and 48 h. Blots were hybridized with acetylated α -tubulin, α - and β -tubulin antibody. GAPDH was used as a loading control. **b** Tubulin

mRNA expression in H460 cells treated with S516 (5, 10, and 20 nM) for 2–24 h. **c** Analysis of change in microtubules by immunocytochemistry from H460 cells treated with S516

First introduced into clinical oncology in the 1960s, microtubule target agents (MTAs) are essential components in the therapy of many cancers [12]. Tubulin polymerization inhibitors act primarily by disrupting the tubulin network of the endothelial cell cytoskeleton, leading to shape changes and increased vascular permeability. Our *in vitro* study results provide supportive evidence of increased tumor vascular damage following S516 treatment. S516 reduced the protein level on both the supernatant liquid (isolated tubulin, S) and the sediment (polymerized tubulin, P) by immunoblot using H460 cells (Fig. 3) and HUVECs (Fig. 6a). S516 reduced the total amount of microtubules depending on concentration, as shown by confocal imaging (Figs. 4c and 6d). These results

support the view that S516 is a novel VDA. Tubulin mRNA expression was also reduced at a time point that was different from protein level in S516-treated cells (Figs. 4b and 6c).

The regulation of tubulin expression remains largely unexplored. The first model proposed to explain the regulation of tubulin expression was based on an autoregulatory mechanism, in which soluble tubulin pools regulate the rate of mRNA transcription. Cleveland et al. reported that the tubulin soluble level not only modulates the rate of tubulin synthesis, but also modulates the response to depolymerization [21]. This is due to the MREI sequence common to all tubulin isotypes. But, this model does not explain variations specific for each tubulin isotype.

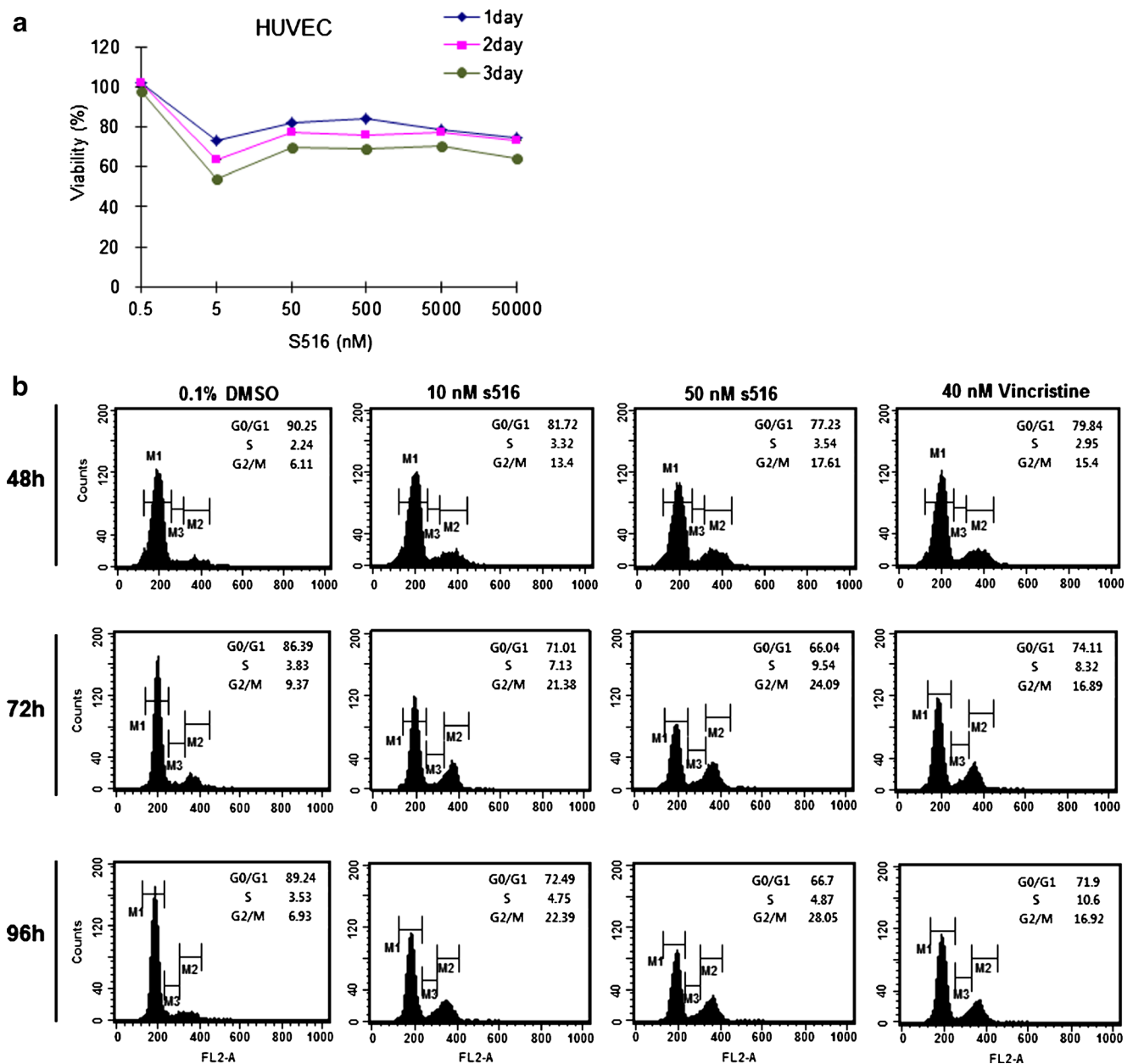


Fig. 5 Effect of S516 on HUVECs growth and G₂/M arrest. **a** To show the inhibitory effects of S516 on the cell proliferation, exponentially growing cells were treated with the indicated concentrations of S516 for 24 h, 48 h and 72 h, and cell proliferation was assessed using MTS reagent. Cytotoxic effect of S516 was increased in a time-dependent manner. **b** To observe the cell cycle arrest by S516, HUVECs were

treated either 0.1 % DMSO (control) or each concentration of S516 and paclitaxel for 24 h, 48 h and 72 h. Cells were analyzed by flow cytometry and the percentage of cells in each phase of the cell cycle was analyzed using flow cytometry. The analysis showed increased G₂/M phase in 50 nM S516-treated cells

Since both mRNA and protein level of tubulin were reduced, our results may not support an autoregulatory mechanism hypothesis. Another mechanism of tubulin regulation is related with drug resistance. For example, Taxol or vinca alkaloid increases mRNA expression of class I, III and IVa tubulin isotypes in drug-resistant tumors [22–26]. Therefore, we also confirmed mRNA expression of tubulin isotypes (class I, II, III, IVa and VI). No changes were evident (data not shown).

Overall, our data suggest that the quantitative change of tubulin proteins reflected a change in the level of the protein. The quantitative change of protein and mRNA occurred independent of each other.

We also evaluated the anti-tumor efficacy of gemcitabine in combination with CKD-516. The sequence of administration should be carefully designed to avoid an effect of one agent with the other. Ideally, a combination of VDAs and cytotoxic agents is expected to take advantage of

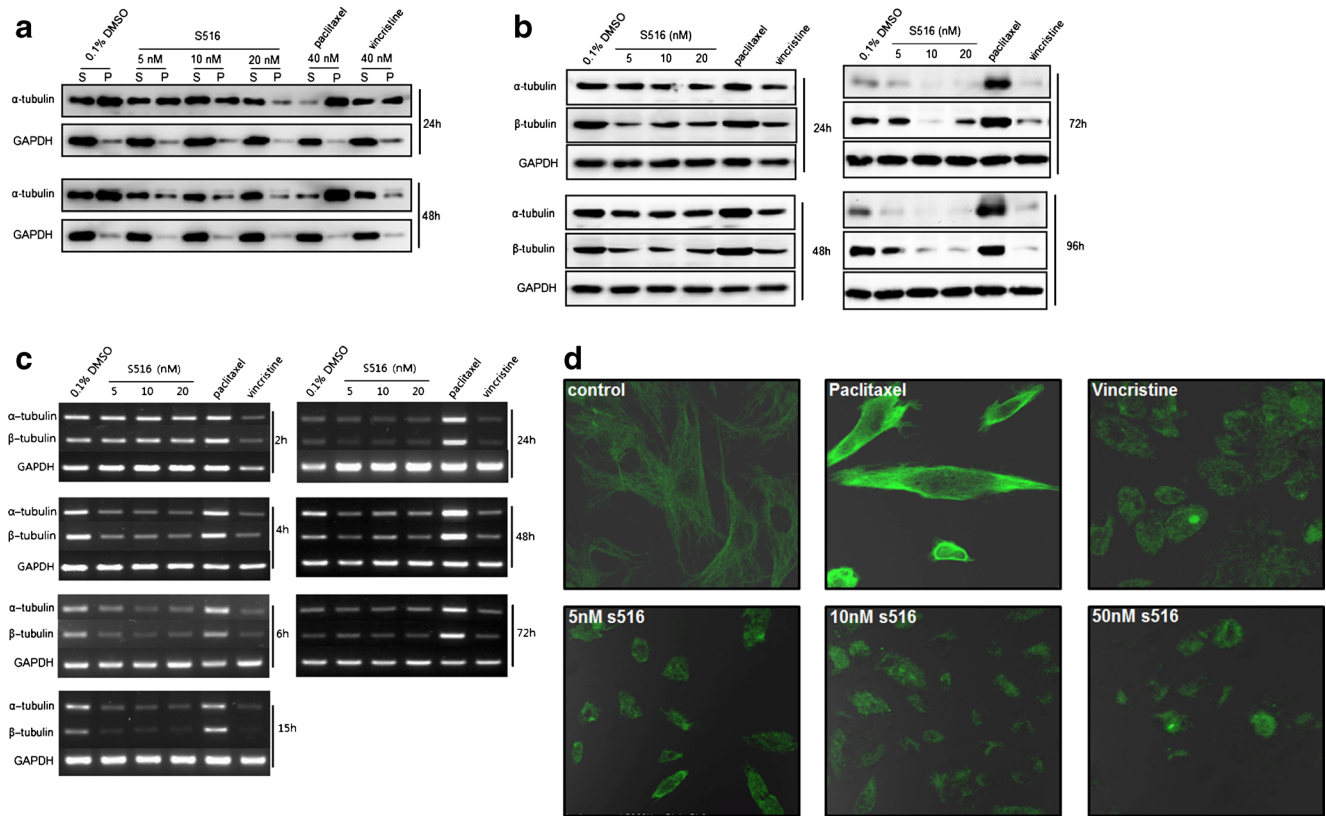


Fig. 6 S516 induces microtubule depolymerization in HUVECs. HUVECs were treated with S516, or DMSO as the control, for indicated times at 5–50 nM. **a** Cell lysates were separated into polymerized (P) or soluble (S) fractions by centrifugation 2,000 rpm at 22 °C for 30 min. Equal volumes were separated by SDS-PAGE and evaluated by immunoblot probed with anti- α -tubulin antibody and anti-GAPDH antibody. **b** Immunoblot of

HUVECs treated with S516 (5, 10 and 50 nM) for indicated times. Blots were hybridized with acetylated α -tubulin, α - and β -tubulin antibody. GAPDH was used as a loading control. **c** Tubulin mRNA expression in HUVECs treated with S516 (5, 10 and 50 nM) for 2–72 h. **d** Analysis of change in microtubules by immunocytochemistry from HUVECs treated with S516. The data are representative of three independent experiments

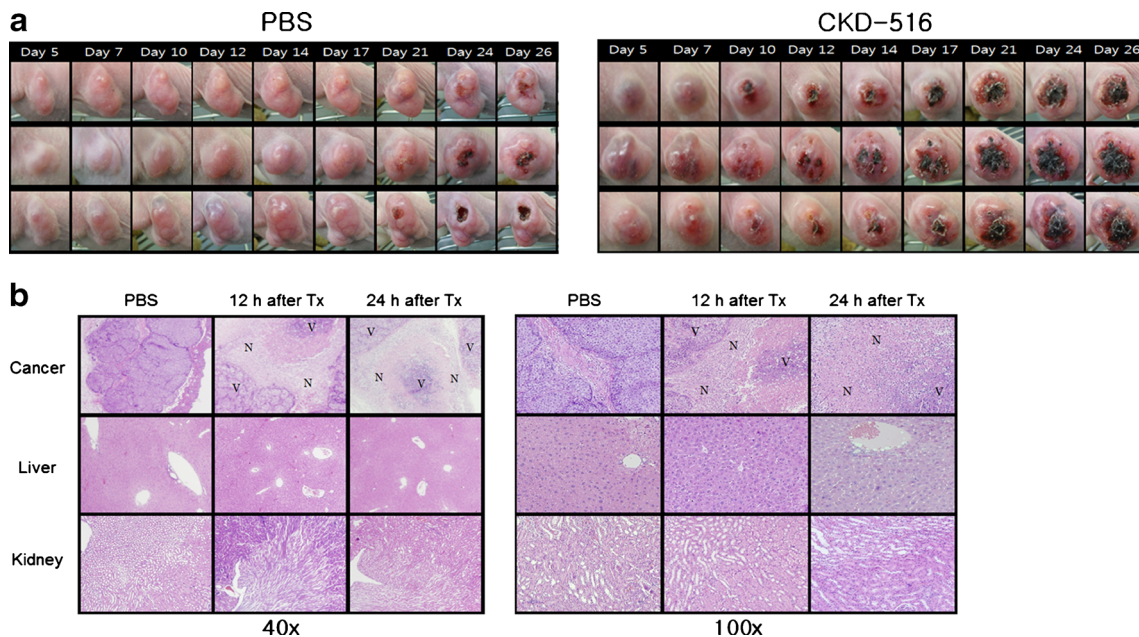
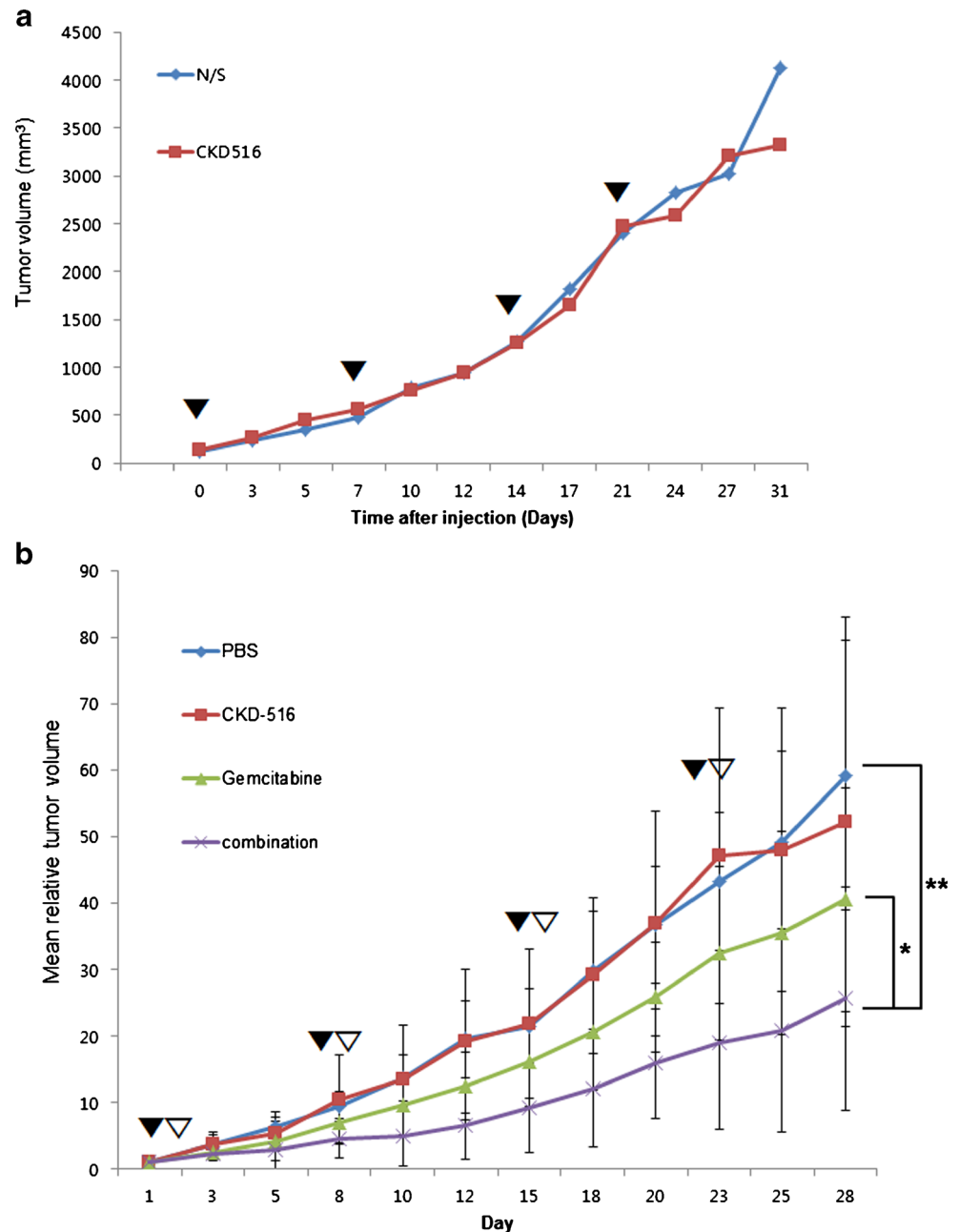


Fig. 7 Gross morphological and histopathological changes. **a** Observation of necrosis in tumors after treatment of CKD-516 in the H460 xenograft model. **b** Histological analysis of tumor tissues ($\times 40$

and $\times 100$) and normal tissues treated with CKD-516. Tumors were excised from H460 xenograft treated with PBS or CKD-516

Fig. 8 Anti-tumor activity of CKD-516 in the H460 xenograft model. **a** CKD-516 alone treatment had no inhibitory effect on tumors in the H460 xenograft model. Control group mice were injected intraperitoneally with saline. CKD-516 group mice were injected with 2.5 mg/kg. All experiment groups were administrated once weekly for 4 weeks. Black arrowheads indicate treatment. **b** Gemcitabine combined with CKD-516 had an additive inhibitory effect in the H460 xenograft model. The experimental groups were divided into one group injected with 100 μ l of gemcitabine at the concentration of 40 mg/kg and a second group was injected with 100 μ l of CKD-516 (2.5 mg/kg) and gemcitabine (40 mg/kg) at defined times. Black (gemcitabine) and white (CKD-516) arrowheads indicate treatment. * P <0.005 compared to gemcitabine, ** P <0.0001 compared to control



the effect of the former on endothelial cells and of the latter on tumor cells. The effects of VDAs on the vasculature have obvious important implications in the design of combination treatments with these agents, given their possible interference with the distribution of the cytotoxic drug [27–29]. Presently, we used the only one route of administration. In the H460 xenograft model, tumor growth was inhibited with gemcitabine alone (33 %) as compared to control. However, xenograft model treated with gemcitabine+CKD-516 showed significant tumor growth delay (57 % and 36 %) as compared to control and gemcitabine alone.

This study demonstrates that CKD-516 is a novel VDA in the H460 xenograft model and enhances antitumor activity in combination with gemcitabine, and suggests an avenue for effective combination therapy in treating solid tumors.

Acknowledgment This work was supported by Priority Research Center Program through the National Research Foundation of Korea (NRF) funded by the Ministry of Education, Science and Technology (2009–0094050) and by grants from Chong Kun Dang Pharmaceutical Corp. in Korea.

Conflict of interest The authors declare that they have no conflict of interest.

References

- Folkman J (1990) What is the evidence that tumors are angiogenesis dependent? *J Natl Cancer Inst* 82:4–6
- Zetter BR (1998) Angiogenesis and tumor metastasis. *Annu Rev Med* 49:407–424
- Eichhorn ME, Kleespies A, Angele MK, Jauch KW, Bruns CJ (2007) Angiogenesis in cancer: molecular mechanisms, clinical impact. *Langenbecks Arch Surg* 392:371–379
- Ergun S, Kilic N, Wurbach JH et al (2001) Endostatin inhibits angiogenesis by stabilization of newly formed endothelial tubes. *Angiogenesis* 4:193–206
- Davidoff AM, Ng CY, Brown P et al (2001) Bone marrow-derived cells contribute to tumor neovasculature and, when modified to express an angiogenesis inhibitor, can restrict tumor growth in mice. *Clin Cancer Res* 7:2870–2879
- Lyden D, Hattori K, Dias S et al (2001) Impaired recruitment of bone marrow-derived endothelial and hematopoietic precursor cells blocks tumor angiogenesis and growth. *Nat Med* 7:1194–1201
- Cushman M, Nagarathnam D, Gopal D, Chakraborti AK, Lin CM et al (1991) Synthesis and evaluation of stilbene and dihydrostilbene derivatives as potential anticancer agents that inhibit tubulin polymerization. *J Med Chem* 34:2579–2588
- Thorpe PE (2004) Vascular targeting agents as cancer therapeutics. *Clin Cancer Res* 10:415–427
- Moon CH, Lee SJ, Lee HY, Song HT, Min YJ et al (2013) KML001 displays vascular disrupting properties and irinotecan combined antitumor activities in a murine tumor model. *PLoS One* 8(1):e53900
- Kavallaris M (2010) Microtubules and resistance to tubulin-binding agents. *Nat Rev Cancer* 3:194–204
- Calligaris D, Verdier-Pinard P, Devred F, Villard C, Braguer D, Lafitte D (2010) Microtubule targeting agents: from biophysics to proteomics. *Cell Mol Life Sci* 67(7):1089–1104
- Jordan MA, Kamath K (2007) How do microtubule-targeted drugs work? An overview. *Curr Cancer Drug Targets* 7(8):730–742
- Lee J, Kim SJ, Choi H, Kim YH, Lim IT et al (2010) Identification of CKD-516: a potent tubulin polymerization inhibitor with marked antitumor activity against murine and human solid tumors. *J Med Chem* 53:6337–6354
- Palazzo A, Ackerman B, Gundersen GG (2003) Cell biology: tubulin acetylation and cell motility. *Nature* 421:230
- Infante AS, Stein MS, Zhai Y, Borisy GG, Gundersen GG (2000) Detyrosinated (Glu) microtubules are stabilized by an ATP-sensitive plus-end cap. *J Cell Sci* 113(Pt 22):3907–3919
- Kanthou C, Tozer GM (2009) Microtubule depolymerizing vascular disrupting agents: novel therapeutic agents for oncology and other pathologies. *Int J Exp Pathol* 90:284–294
- Horsman MR, Siemann DW (2006) Pathophysiologic effects of vascular-targeting agents and the implications for combination with conventional therapies. *Cancer Res* 66:11520–11539
- Ching LM, Goldsmith D, Joseph WR, Kömer H, Sedgwick JD et al (1999) Induction of intratumoral tumor necrosis factor (TNF) synthesis and hemorrhagic necrosis by 5,6-dimethylxanthenone-4-acetic acid (DMXAA) in TNF knockout mice. *Cancer Res* 59:3304–3307
- Joseph WR, Cao Z, Mountjoy KG, Marshall ES, Baguley BC et al (1999) Stimulation of tumors to synthesize tumor necrosis factor- α in situ using 5,6-dimethylxanthenone-4-acetic acid: a novel approach to cancer therapy. *Cancer Res* 59:633–638
- Hammers HJ, Verheul HM, Salumbides B, Sharma R, Rudek M et al (2010) Reversible epithelial to mesenchymal transition and acquired resistance to sunitinib in patients with renal cell carcinoma: evidence from a xenograft study. *Mol Cancer Ther* 9:1525–1535
- Cleveland PF (1983) Elevation of tubulin levels by microinjection suppresses new tubulin synthesis. *Nature* 305:738–740
- Kavallaris M, Kuo DYS, Burkhart CA et al (1997) Taxol-resistant epithelial ovarian tumors are associated with altered expression of specific β -tubulin isotypes. *J Clin Invest* 100:1282–1293
- Kamath K, Wilson L, Cabral F, Jordan MA (2005) β III-tubulin induces paclitaxel resistance in association with reduced effects on microtubule dynamic instability. *J Biol Chem* 280:12902–12907
- Kavallaris M, Tait AS, Walsh BJ et al (2001) Multiple microtubule alterations are associated with Vinca alkaloid resistance in human leukemia cells. *Cancer Res* 61:5803–5809
- Galmardini CM, Kamath K, Vanier-Viorneri A et al (2003) Drug resistance associated with loss of p53 involves extensive alterations in microtubule composition and dynamics. *Br J Cancer* 88:1793–1799
- Arai K, Maruo K, Ara KY, Uehara K, Matsuda H (2001) Characterization of isotype-specific regions of five classes of canine β -tubulin and their expression in several tissues and cell culture. *J Vet Med Sci* 63:1297–1302
- Chaplin DJ, Horsman MR, Siemann DW (2006) Current development status of small-molecule vascular disrupting agents. *Curr Opin Invest Drugs* 7:522–528
- Bouzin C, Feron O (2007) Targeting tumor stroma and exploiting mature tumor vasculature to improve anti-cancer drug delivery. *Drug Resist Updat* 10:109–120
- Patterson DM, Rustin GJ (2007) Vascular damaging agents. *Clin Oncol (R Coll Radiol)* 19:443–456